DRAFT

ROYAL HOLLOWAY UNIVERSITY OF LONDON

M.SC THESIS

STUDENT ID: 100920158

Benchmarking Simulations of Slow Extraction Driven By RF Transverse Excitation at the CERN Proton Synchrotron[1]

Author:
Thomas BASS

Supervisor:
Professor Stephen GIBSON

May 31, 2023

DRAFT

Contents

DRAFT

ABSTRACT

Resonant slow extraction is a beam extraction method which provides a continuous spill over a longer duration than can be achieved with fast single-turn or non-resonant multi-turn extraction. By using transverse excitation to drive the circulating particles onto the resonance, a beam can be delivered to fixed target experiments which require long-duration spills.

In order to accurately and efficiently simulate the extraction process over a wide range of timescales, new modelling tools and computing platforms must be explored. By utilising optimised computational hardware - such as General Purpose Graphics Processing Units (GPGPUs), and next-generation simulation software (such as Xsuite), computation times for simulations can be reduced by several orders of magnitude.

This thesis presents recent developments of resonant slow extraction modelling and benchmarking with a comparison to measurements made at CERN's Proton Synchrotron (PS), with a particular focus on understanding the dynamics of transverse RF excitation and effect on spill quality.

Chapter 1

Introduction

The CERN Proton Synchrotron (PS), alongside providing intermediary acceleration for hadron and ion beams for the Super Proton Synchrotron (SPS) and eventually the Large Hadron Collider (LHC), provides beams for the many fixed target experiments located at the East Area (EA) experimental facility. This facility, as illustrated in chapter 1, consists of the proton (IRRAD) and mixed-field (CHARM) irradiation facilities, via a dedicated $24\,\mathrm{GeV/c}$ beamline, in addition to a multi-target beamline providing three secondary beams.

Ongoing experiments in these facilities such as the CHARM High-energy Ions for Micro Electronics Reliability Assurance (CHIMERA) [1] use high-Z ions (Pb) to simulate the harsh radiation environment of cosmic rays which satellites experience. Using low-intensity ($<10^6\,\mathrm{ions/spill}$), high-energy ($>100\,\mathrm{MeV/u}$) beams, customers such as the European Space Agency can assess the reliability of new materials in these environments. Figure 1 illustrates the two injection chains of the PS, either with Lead Ions sourced from the Linear Accelerator 3 (Linac3) and Low Energy Ion Ring (LEIR) chain, or Protons from the Linac4 and the Proton Synchrotron Booster (PSB).

1.1 Motivation

The CHIMERA experiment, and other experiments located at the East Area and its SPS-sister-site North Area, are referred to as fixed-target experiments, to distinguish them from the collision experiments for which the LHC is most famous. The nature of these fixed-target experiments requires that a semi-continuous beam is delivered: if the entire energy of the PS was delivered to a material sample, for example, in an effectively

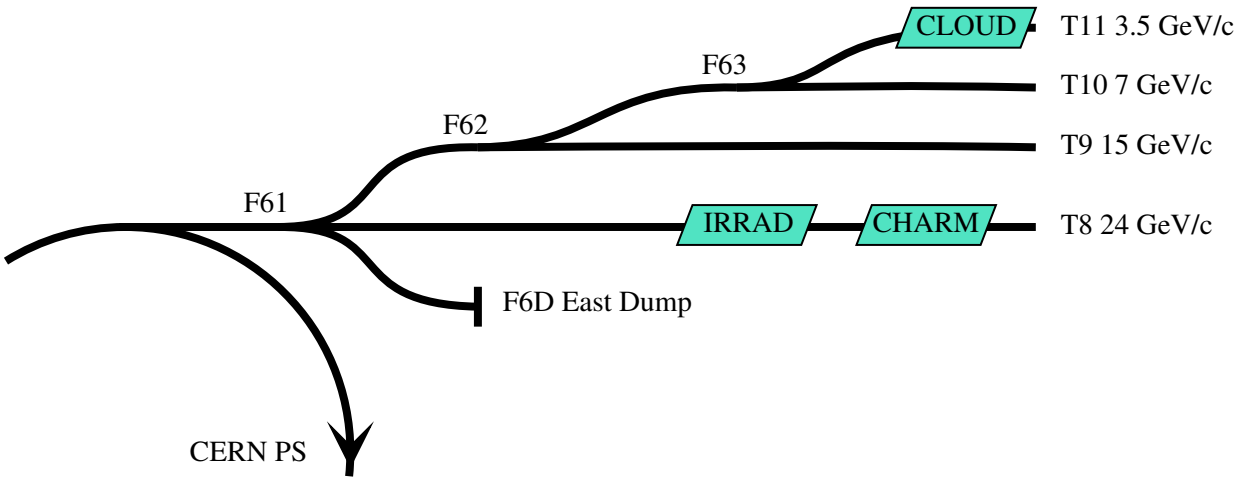

Figure 1.1: Layout diagram of the CERN East Area (EA) beamlines, their energies, and experiments.

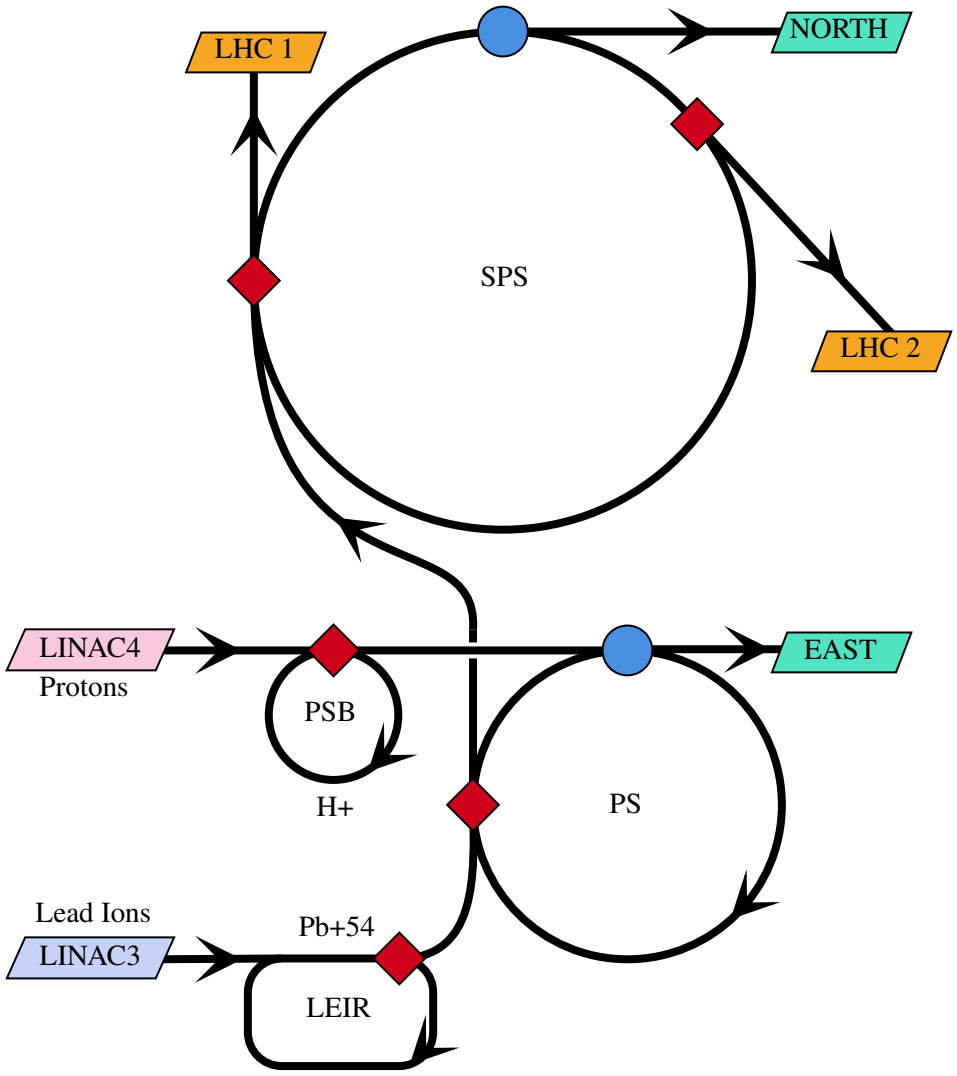

Figure 1.2: Layout diagram of the primary acceleration chain at CERN. Particles are sourced from either Linac 3 (for Lead ions) or Linac4 (for Protons), and accelerated through the LEIR or PSB respectively. After injection and acceleration in the PS, beams are extracted either to the SPS or East Area (EA). Particles at the SPS are either extracted at two LHC extraction locations, or towards the North area. Red diamonds mark Fast extraction locations, and blue circles mark Slow extraction regions.

instantaneous "spill" (a controlled removal of particles from the circular accelerator), any sensitive acquisition equipment would become saturated, and the fixed target itself likely destroyed. With the PS's revolution frequency typically around $470\,\mathrm{kHz}$, delivering particles over the period of one turn could, at most, provide a spill time on the order of $2\,\mu\mathrm{s}$. This extraction method, known as "fast" extraction, is commonly used to transfer particles between successive accelerators, where the bunched time-structure of the beam must be preserved. To provide spills on the order of $\sim 100\,\mathrm{ms}$ required for these experiments, a "slow" extraction system is employed.

1.1.1 Performing Slow Extraction

1. Outlines the motivation behind performing Slow Extraction
2. Slow extraction is used where a spill has to be significantly longer than the revolution frequency
3. This has particular applications in medical and electronic reliability. Time structure is key
4. *Medical: its important to control dosage extremely precisely (why?)
5. Electronics reliability: CHIMERA STATUS https://indico.cern.ch/event/1116677/contributions/4695314/attachments/2400040/4104314/CHIMERA%20status%20and%20outlook.pdf

To move particles between successive accelerators along the primary CERN acceleration chain, the PSB, PS, and SPS are equipped with fast extraction systems. The theory and methodology of these processes will be fully explored in the next section, but a general overview and understanding of its benefits and disadvantages can help motivate the use of *slow* extraction.

As previously mentioned, fast extraction provides a spill of particles typically over the duration of one turn. A strong magnet, at a suitable location in the machine, imparts a large "outwards" (away from the centre of revolution) deflective force to a bunch of particles. This ejects the particle bunch from the nominal orbit trajectory, where it encounters a second magnet—called a septum—to align the particle bunch along a transfer line. The opposite effect is then used to inject the bunch into the next machine: a magnet "kicks" the particles onto the circulating beam trajectory.

This general method of fast *single-turn* extraction is performed at two locations in the SPS—Long Straight Sections (LSS) 4 and 6—to fill the two counter-rotating beamlines in the LHC [2]. The PSB performs similar extraction, but has the added complexity of "merging" four seperate stacked accelerators to one transfer line [3]. LEIR likewise performs fast extraction [4]. The general layout of these systems are shown in 1, where red diamonds mark fast extraction locations. Fast extraction systems are also used at the beam dump facilities at various stages of the accelerator chain.

In accelerator-to-accelerator contexts, the synchronous nature of fast extraction allows particles to remain bunched. Multi-turn fast extraction extends this benefit, and is performed when filling the SPS for its fixed-target experiments (North Area) from the PS. As the SPS ($6.9\,\mathrm{km}$) is almost approximately 11 times longer in circumference than the PS ($628\,\mathrm{m}$)[1], the entire SPS can be filled by 11 successive extractions of the full PS. This method, coined as *continuous transfer* (CT)

In order to provide a long-duration spill, *slow extraction* must be used. Where fast extraction and injection methods utilise kicker magnets to move entire particle bunches between successive accelerators, slow extraction regimes rely on manipulating the beam to extract a small fraction of the available particles over a large number of turns. This regime produces the desired spill, but can be very sensitive to small changes of parameters. Accurately simulating the entire extraction process can often take tremendous processing power, as each of the 10^{12} particles need to be tracked for many thousands of turns.

Therefore, to accurately simulate the spill produced by these extraction methods, one must first understand the fundamentals of accelerator beam dynamics, and grasp the technical challenges faced with simulation efforts. This thesis will first construct the required dynamic system of particle motion in a circular accelerator, and then introduce the theory behind slow extraction and the method used in this paper. Establishing a

[1] The PS is 100 meters across, and therefore $200\pi\mathrm{m}$

motivation for accurate and fast simulations slow extraction, various simulation methods will be presented, compared, and benchmarked with real-world data taken with the CERN PS.

1.1.2 Simulating Slow Extraction

1. Outlines the motivation behind *simulating* SX
2. Long spills can be sensitive to small changes in conditions - understanding these is important
3. Many small/medical accelerators have high machine-on time and low machine demand, meaning they can test on accelerator rather than simulate
4. Smaller/medical accelerators tend to also be physically simpler
5. This is not afforded to CERN - many users competing for availability, highly complex system

1.2 Challenges

1. Outlines the *challenges* with simulating SX
2. Simulating Fast extraction is well understood, as numerical models are easier (why? example?)
3. Simulating Fast extraction can typically happen over a very small number of turns
4. - Describe how Fast Extraction works optically
5. - Provide an example: fast extraction at CERN SPS to LHC https://cds.cern.ch/record/2674120/files/488.pdf

Chapter 2

Theory

2.1 Single-Particle Transverse Beam Dynamics

2.1.1 Coordinate System

The coordinate systems used to describe the dynamic motion of particles in a particle accelerator such as the PS relies on the periodic nature of a circular accelerator. Using a traditional Cartesian x, y, z coordinate system would quickly introduce complications when describing circular trajectories, and so a local curvilinear coordinate system is used.

The basis vectors for this system, $(\hat{x}, \hat{y}, \hat{s})$, constantly rotate in Cartesian space as the reference particle moves along the orbit of the accelerator. The longitudinal vector $\hat{s}$ is tangent to the particle's orbit, and the $\hat{x}$ direction is parallel to the radius of the accelerator. The absolute direction of $\hat{y}$ does not change, but makes one complete rotation in one closed orbit of the reference particle through the accelerator. This system is shown in Figure 2.1, along with the radius of the circular trajectory ρ, and the angle from the origin $s = 0$.

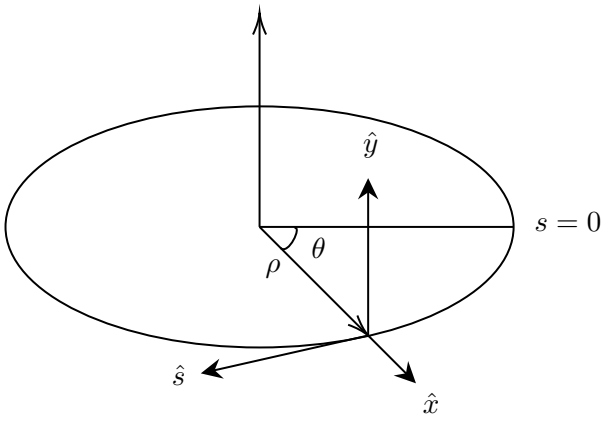

Figure 2.1: The *Frenet-Serret* vectors used to define the coordinate system used in particle beam dynamics.

This coordinate system is academically known as a *Frenet-Serret* type coordinate system, and can be rigorously defined by the unit vector *tangent* to the curve $\hat{T}$ (pointing in the direction of motion), the unit vector *normal* to the tangent and on the tangential plane $\hat{N}$, and the binormal unit vector $\hat{B}$, the cross product of $\hat{T}$ and $\hat{N}$. These unit vectors, forming an orthonormal basis spanning $\mathbb{R}^3$, and known collectively as the

TNB frame, are equal to the vectors $\hat{x}, \hat{y}, \hat{s}$ by:

$$\begin{pmatrix} \hat{T} \\ \hat{N} \\ \hat{B} \end{pmatrix} = \begin{pmatrix} \hat{s} \\ -\hat{x} \\ \hat{y} \end{pmatrix} \quad \text{Eq. 2.1}$$

The coordinate system $(\hat{x}, \hat{y}, \hat{s})$ relies on the right-hand chirality (Figure 2.2) of the vector cross product for the $\hat{x}$ vector to point radially outwards from the centre of the machine, the $\hat{y}$ vector points upwards, and the $\hat{s}$ vector points in the direction of motion. The direction of $\hat{x}$ to point outwards from the centre of revolution is chosen as injection and extraction line apertures will therefore be located in the positive $\hat{x}$.

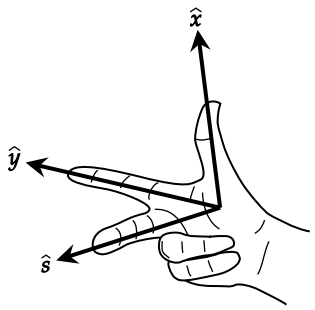

Figure 2.2: The right-hand chirality rule defining the direction of $\hat{s} = \hat{x} \times \hat{y}$

2.1.2 Variable Space

1. 6D space fully describes particles
2. 4D space describes transverse motion - can be understood separately
3. Differences in variables between simulation software

2.1.3 Ring Geometry

Lorentz force balances centrifugal force - understanding of beam rigidity

1. Design orbit created by dipoles
2. Focussing created by quadrupoles
3. Non-Linear effects created by Sextupoles

All descriptions of particle accelerators are build upon the Lorentz force, describing the force $\vec{F}$ acting on a charged particle with charge q as it moves through an electric field $\vec{E}$ and magnetic field $\vec{B}$ with velocity $\vec{v}$, given as

$$\vec{F}_{\text{lorentz}} = q \cdot (\vec{E} + \vec{v} \times \vec{B}) \quad \text{Eq. 2.2}$$

This equation can already show why magnetic fields are used in almost all areas of particle acceleration, and not electric fields; a particle with higher velocity v will experience a greater force from a constant magnetic field $\vec{B}$, whereas the contribution from the electric field $\vec{E}$ will remain constant. Therefore, at velocities approaching the speed of light ($v \to c$), we can begin to neglect $\vec{E}$ for some derivations.

The other force experienced by a particle in an accelerator is the centripetal[1] force:

$$\vec{F}_{\text{centrif.}} = \frac{m_0 v^2}{\rho} \quad \text{Eq. 2.3}$$

[1]while the coordinate system used allows for a reference frame whose orientation follows the orbit, this frame is not co-moving with the particles, but still fixed in the "laboratory" frame - otherwise, complex Lorentz transformations would be required.

where m_0 is the particle's rest mass, and ρ is the radius of the particle's orbit inside the accelerator.

Equating equations 2.3 and 2.2 yields

$$B\rho = \frac{p}{q} \qquad \text{Eq. 2.4}$$

The quantity $B\rho$ is known as the momentum rigidity of a beam, and defines the bending angle of a particle for a given magnetic field.

If the momentum $p = mv$ of the particle is measured in $\mathrm{GeV}/c_0/\mathrm{amu}$, and A and Ze are the atomic mass number and charge of the particle, the momentum rigidity can be expressed in Tesla-meters:

$$B\rho\ [\mathrm{T\,m}] = \frac{p}{q} = \frac{A}{Z} \times 3.33564 \times q\ [\mathrm{GeV}/(c_0\,\mathrm{u})] \qquad \text{Eq. 2.5}$$

However, this formulation only describes a single magnetic field. In order to bend the particles along a circular trajectory, dipole magnets are used to create near-constant fields through which the particles travel. Again referring to Equation 2.2 (with the help of Figure 2.2), a magnetic field pointed vertically upwards (along the $\hat{y}$ vector) will cause a particle with motion along the $\hat{s}$ vector to experience a bending force along the $-\hat{x}$ direction.

The arrangements of these bending magnets - referred to as Main Units (MU) - will define the closed loop of one orbit in the accelerator - the *design orbit*.

If α is the bending angle of a single MU, then α can be related to the momentum rigidity by

$$\alpha = \frac{ds}{\rho} = \frac{B\ ds}{B\rho} \qquad \text{Eq. 2.6}$$

Integrating this over all magnets in the ring, therefore, must be equal to one full revolution, 2π

$$\frac{\int B\ ds}{B\rho} \equiv 2\pi \qquad \text{Eq. 2.7}$$

This result may seem obvious, but it is an important step in understanding why the transverse motion (i.e. that in the $\vec{x}$ and $\vec{y}$ directions) can be understood and analysed separately from that of the longitudinal ($\vec{s}$) motion. This result also provides one of the first key insights which is not obvious at first - that "circular" accelerators are in fact n-sided polygons, with bending magnets at each vertex, and a *drift* (accelerator sections without any significant electromagnetic field) or other non-bending multipole magnet at each side: in the case of the LHC, 1,232 dipole magnets are used to keep the beam on it's circular path; in the PS - 100.

While the arrangement of these magnets - referred to as the *lattice* - is intended to create the design orbit, alignment errors, instabilities, and non-linearities create the actual closed-loop orbit of the machine - the *reference orbit*.

is it more correct to say that the quadrupoles are *part* of the MUs? or are the MUs just the dipoles and separate from focussing?

2.2 Multi-particle Transverse Beam Dynamics

While the configuration of the MU bending magnets, in addition to drifts and other higher-order magnets (discussed shortly), defines the design orbit of a single ideal particle, an accelerator beam is comprised of a great number of particles grouped together into one *bunch* - on the order of 10^{12} for the PS. These particles naturally have small variations in their initial position, angle, and momenta. The evolution of these changes in position and angle, with respect to the reference orbit, is understood through separating the longitudinal motion from motion in the transverse plane.

In the transverse dynamics of an accelerated beam, the *betatron function* refers to one of the three functions (α, β, and γ), which, along with betatron phase μ, can provide an emittance-independent representation

of the properties of the beam. These functions are known as the *Twiss* or *Courant-Snyder* parameters of a transverse dynamics system. In a periodic (circular) accelerator, the linear equation for transverse equation takes the form of a Hill differential equation:

$$\frac{d^2x}{ds^2} - K(s) \cdot x(s) = 0 \qquad \text{Eq. 2.8}$$

where x is the transverse displacement as a function of longitudinal position s, and K is the focussing coefficient. Following Floquet's theorem [5], general solution to this equation takes the form of the harmonic oscillator

$$x(s) = \sqrt{\varepsilon}\sqrt{\beta(s)}\cos(\varphi(s) - \varphi_0) \qquad \text{Eq. 2.9}$$

where φ is the phase of oscillation, φ_0 is the initial condition, ε is an invariant property of the ensemble of particles (emittance), and $\beta(s)$ is an amplitude function. Taking the derivative with respect to s gives an equation for the angle of the trajectory:

$$x'(s) = \sqrt{\varepsilon}\sqrt{\beta(s)}\left(\frac{1}{2}\beta'(s)\cos(\varphi(s) - \varphi_0) + \sin(\varphi(s))\right) \qquad \text{Eq. 2.10}$$

From these solutions, we can obtain an equation to describe phase advance of the oscillation:

$$\varphi(s) = \int_0^s \frac{ds}{\beta(s)} \qquad \text{Eq. 2.11}$$

Basic analysis of this equation shows that at locations with large β amplitude (and thus a large transverse displacement), phase advance φ is small, and vice versa. The number of transverse oscillations per turn, the *tune* of the machine, is therefore defined as

$$Q = \frac{1}{2\pi}\oint \frac{ds}{\beta(s)} \qquad \text{Eq. 2.12}$$

Momentum compaction factor

Gamma factor

Transverse tune = betatron tune

Long tune = synchrotron tune

Normalised emittance is constant under adiabatic damping

2.2.1 Multi-particle Transverse Dynamics

1. 1. Relativistic beta, gamma
2. Twiss, momentum compaction, emittance, constant emittance (e.g. adiabatic damping)
3. How tune emerges, Adiabatic tune changes

2.2.2 Multi-particle Longitudinal Dynamics

1. Tomography and Tomoscope
2. Longitudinal Emittance

2.3 Slow Extraction

1. Machine resonance at third order, leading to a derivation of the Kobayashi Hamiltonian and Steinbach diagram
2. COSE (chromatic)

3. Q-sweep
4. Betatron
5. **RFKO** INTRODUCE RFKO FORMALLY HERE
6. Mathematical description of the four regimes
7. Perform these four extraction regimes
8. Demonstrate why RFKO is of interest

An analysis of RFKO begins with understanding transverse resonance effects in an accelerator. Particles which start with non-zero initial conditions are subject to transverse oscillations as they progress longitudinally - this is known as *betatron* oscillation. A consequence of this oscillation is that particles at different transverse positions will experience different bending (dipole) and focussing (quadrupole) forces due to fringe fields or errors in magnets. This leads to an energy spread in the machine. A *multi-energetic* beam will therefore have a spread of momenta, referred to as $dp - d - p_0$, the relative momentum deviation. A particle with $dp > 0$ will require an orbit with large radius, and vica-versa.

It is easily understood that magnets of order n create instabilities at the n^{th} order tune. We start with an understanding of how slight variations in initial conditions of a beam causes dispersion. With reference to an *equilibrium orbit* (an orbit which passes through the exact centre of all dipoles and quadrupoles), a range of initial position distributions will cause particles at different spatial coordinates to experience different forces from magnets. This leads to a transverse oscillation around the equilibrium orbit which we understand as *betatron oscillation*, with the tune Q of a machine being the number of betatron oscillations completed per revolution.

This "energy spread" necessarily leads to a momentum spread, which we understand as either purely relative or normalised deviation from the equilibrium momentum p_0:

$$dp = p - p_0; \ \frac{dp}{p_0} = \frac{p - p_0}{p} \qquad \text{Eq. 2.13}$$

We already understand that the particle's trajectories are defined by a differential equationCITE, which takes the form of

$$\frac{d^2x}{ds^2} + K(s)x = \frac{1}{\rho}\frac{\Delta p}{p_0} \qquad \text{Eq. 2.14}$$

where $K(s)$ the normalised quadrupole strength;

$$K(s) = -\left(k(s) - \frac{1}{\rho(s)^2}\right) \qquad \text{Eq. 2.15}$$

$\frac{1}{\rho}$ is the dipole strength (the reciprocal of the equilibrium radius). The solution to this equation is the sum of the general and particular solutions, the first of which.

Chapter 3

Simulation and Benchmarking

3.1 Simulation Methodology

Focussed on original contribution

1. What tools are available? MAD-X, MapTrack, Henontrack, Xsuite
2. How do they compare? Accuracy studies between basic simulations
3. How extraction can be implemented in them: MAD-X limitation of sub-turn frequencies; Xtrack Exciter element
4. How extraction compares spill accuracy studies between simulations and machine data
5. How performance compares performance studies between SX simulations on CPU and GPGPU

Chapter 4

Conclusion

Chapter 5

Acknowledgements

Chapter 6

Bibliography

Bibliography

[1] M. Fraser, P. A. Arrutia Sota, K. Biłko, N. Charitonidis, S. Danzeca, M. Delrieux, M. Duraffourg, N. Emriskova, L. S. Esposito, R. García Alía, A. Guerrero, O. Hans, G. Imesch, E. Johnson, G. Lerner, I. Ortega Ruiz, G. Pezzullo, D. Prelipcean, F. Ravotti, F. Roncarolo, and A. Waets, "Feasibility of Slow-Extracted High-Energy Ions From the CERN Proton Synchrotron for CHARM," *JACoW IPAC*, vol. 2022, pp. 1703–1706, 2022. [Online]. Available: https://cds.cern.ch/record/2845894

[2] M. A. Fraser, "Fast extraction: single and multi-turn," *CERN Yellow Reports: School Proceedings*, vol. Vol 5, p. Extraction and Transfer, 2018. [Online]. Available: https://e-publishing.cern.ch/index.php/CYRSP/article/view/703

[3] K. D. Metzmacher and L. Sermeus, "The PSB Ejection and Recombination Kicker Systems for LHC," CERN, Geneva, Tech. Rep., 2000. [Online]. Available: http://cds.cern.ch/record/2061508

[4] S. Ghithan, G. Roy, and S. Schuh, "Design study of beam transport lines for BioLEIR facility at CERN," *JINST*, vol. 12, no. 09, p. P09019, 2017.

[5] J. Rossbach and P. Schmüser, "Basic course on accelerator optics," 1994. [Online]. Available: http://cds.cern.ch/record/247501

[6] H. Wiedemann, *Particle Accelerator Physics*. Springer International Publishing, 2015. [Online]. Available: https://doi.org/10.1007/978-3-319-18317-6

[7] W. Hillert, "Transverse linear beam dynamics," 2021. [Online]. Available: https://arxiv.org/abs/2107.02614

[8] G. Russo, "Radio frequency knockout (rfko) extraction: Hardware analysis and beam optics simulation and optimization," Mar 2019. [Online]. Available: https://webthesis.biblio.polito.it/10253/

[9] S. Savazzi *et al.*, "Implementation of RF-KO Extraction at CNAO," in *Proc. 10th International Particle Accelerator Conference (IPAC'19), Melbourne, Australia, 19-24 May 2019*, ser. International Particle Accelerator Conference, no. 10. Geneva, Switzerland: JACoW Publishing, Jun. 2019, paper THPMP010, pp. 3469–3471, https://doi.org/10.18429/JACoW-IPAC2019-THPMP010. [Online]. Available: http://jacow.org/ipac2019/papers/thpmp010.pdf

[10] "Xsuite." [Online]. Available: xsuite.web.cern.ch

[11] "Cern optics repository." [Online]. Available: https://acc-models.web.cern.ch/acc-models/

[12] P. Virtanen, R. Gommers, T. E. Oliphant, M. Haberland, T. Reddy, D. Cournapeau, E. Burovski, P. Peterson, W. Weckesser, J. Bright, S. J. van der Walt, M. Brett, J. Wilson, K. J. Millman, N. Mayorov, A. R. J. Nelson, E. Jones, R. Kern, E. Larson, C. J. Carey, İ. Polat, Y. Feng, E. W. Moore, J. VanderPlas, D. Laxalde, J. Perktold, R. Cimrman, I. Henriksen, E. A. Quintero, C. R. Harris, A. M. Archibald, A. H. Ribeiro, F. Pedregosa, P. van Mulbregt, and SciPy 1.0 Contributors, "SciPy 1.0: Fundamental Algorithms for Scientific Computing in Python," *Nature Methods*, vol. 17, pp. 261–272, 2020.

[13] J. Duplissy, F. Hahn, U. Reichl, P. M. Winkler, E. Pedersen, V. Makhmutov, Y. Viisanen, M. Kulmala, M. Wilhelmsson, E. Weingartner, M. Avngaard, J. Curtius, R. Veenhof, L. Laakso, S. Gagne, R. G. Harrison, M. Sipila, A. David, J. H. Seinfeld, T. Nieminen, B. Verheggen, K. L. Aplin, F. Stratmann, F. Arnold, J. Makela, B. Kellett, B. Fastrup, N. D. Marsh, M. Lockwood, K. Carslaw, G. Wehrle, H. Aufmhoff, J. O. P. Pedersen, U. Baltensperger, A. Onnela, A. Laaksonen, M. B. Enghoff,

J. Svensmark, H. Wex, E. Lillestol, P. E. Wagner, J. Kirkby, Y. Stozhkov, J. Polny, T. Bondo, R. Bingham, and H. Svensmark, "Results from the CERN pilot CLOUD experiment," *Atmos. Chem. Phys.*, vol. 10, no. 4, pp. 1635–1647, 2010. [Online]. Available: http://cds.cern.ch/record/1359385

[14] CERN, "Cern yellow reports: School proceedings, vol 5 (2018): Proceedings of the cas-cern accelerator school on beam injection, extraction and transfer," 2018. [Online]. Available: https://e-publishing.cern.ch/index.php/CYRSP/issue/view/62

[15] G. Russo, "Radio frequency knockout (rfko) extraction: Hardware analysis and beam optics simulation and optimization," Mar 2019. [Online]. Available: http://webthesis.biblio.polito.it/id/eprint/10253

[16] V. Nagaslaev, J. Amundson, J. Johnstone, C. Park, and S. Werkema, "Third integer resonance slow extraction using rfko at high space charge." 2011. [Online]. Available: https://accelconf.web.cern.ch/IPAC2011/papers/thps058.pdf

[17] G. Feldbauer, M. Benedikt, and U. Dorda, "Simulations of Various Driving Mechanisms for the 3rd Order Resonant Extraction from the MedAustron Medical Synchrotron," 2011. [Online]. Available: https://cds.cern.ch/record/1379901

[18] G. Sterbini, A. Blas, and S. Gilardoni, "Beam-based Performance of the CERN PS Transverse Feedback," p. MOPAB10, 2015. [Online]. Available: https://cds.cern.ch/record/2158994

[19] E. Métral, G. Arduini, F. Arnold Malandain, W. Höfle, and D. Manglunki, "Controlled Transverse Emittance Blow-up in the CERN SPS," 2010. [Online]. Available: https://cds.cern.ch/record/1208359

[20] P. A. Arrutia Sota, P. Burrows, A. De Franco, M. Fraser, B. Goddard, V. Kain, F. Kuehteubl, M. Pivi, D. Prokopovich, and F. Velotti, "Implementation of a Tune Sweep Slow Extraction with Constant Optics at MedAustron," *JACoW IPAC*, vol. 2022, pp. 1715–1717, 2022. [Online]. Available: https://cds.cern.ch/record/2845862

[21] M. Pari, F. M. Velotti, M. A. Fraser, V. Kain, and O. Michels, "Characterization of the slow extraction frequency response," *Phys. Rev. Accel. Beams*, vol. 24, no. 8, p. 083501, 2021. [Online]. Available: https://cds.cern.ch/record/2780495

[22] K. Okamura, Y. Arakaki, T. Kimura, S. Murasugi, R. Muto, Y. Shirakabe, M. Tomizawa, and E. Yanaoka, "A consideration on the transfer function between rq field and slow extraction spill in the main ring of j-parc," *Proceedings of the 10th Int. Particle Accelerator Conf.*, vol. IPAC2019, p. Australia, 2019. [Online]. Available: http://jacow.org/ipac2019/doi/JACoW-IPAC2019-WEPMP008.html

[23] V. Agoritsas, "Secondary emission chambers for monitoring the CERN Proton Synchrotron ejected beams. Secondary emission chambers for monitoring the CPS ejected beams," 1968. [Online]. Available: https://cds.cern.ch/record/299104

[24] P. Actis, T. Dorenbos, and C. Johnson, "An optically coupled differential beam time structure monitor for slow extraction," CERN, Geneva, Tech. Rep., 1976. [Online]. Available: https://cds.cern.ch/record/2831368

[25] E. P. Johnson *et al.*, "Beam delivery of high-energy ion beams for irradiation experiments at the CERN Proton Synchrotron," ser. International Particle Accelerator Conference, no. 14. JACoW Publishing, Geneva, Switzerland, paper MOPA115, presented at IPAC'23, Venice, Italy, May. 2023, paper MOPA115, this conference.

[26] S. Deghaye, D. Jacquet, J. Kozar, and J. Serrano, "Oasis: A New System to Acquire and Display the Analog Signals for LHC," 2003. [Online]. Available: http://cds.cern.ch/record/693174

[27] M. Gasior and R. Jones, "High Sensitivity Tune Measurement by Direct Diode Detection," 2005. [Online]. Available: https://cds.cern.ch/record/895142

[28] "High throughput condor (htcondor)." [Online]. Available: https://research.cs.wisc.edu/htcondor

Appendix A

Derivations

A.1 Relating longitudinal variables

In order to relate the dispersive and chromatic functions produced by `MAD-X` to those calculated by `Xtrack`, we must multiply `MAD-X`'s results by the relativistic Lorentz factor $\beta = v/c$. This is because `MAD-X` uses the relative momentum error δ_p as a longitudinal variable, defined as

$$\delta_p = \frac{p - p_0}{p_0} \qquad \text{Eq. A.1}$$

, where p is the momentum of the particle, and p_0 the momentum of the *reference* (or *design*) particle, whereas `Xtrack` uses the relative energy error

Appendix B

Code Snippets

Appendix C

Data and Plots